

# Dark soliton dynamics in Bose-Einstein condensates at finite temperature

B. Jackson, N. P. Proukakis, and C. F. Barenghi

*School of Mathematics and Statistics, University of Newcastle upon Tyne, NE1 7RU, United Kingdom*

(Dated: August 23, 2018)

The dynamics of a dark soliton in an elongated Bose-Einstein condensate at finite temperatures is studied using numerical simulations. We find that in the presence of harmonic confinement the soliton may oscillate even at finite temperatures, but with an amplitude that increases with time, indicating the decay of the soliton. The timescale of this decay decreases both with increasing temperature and with increasing initial soliton velocity. Simulations performed for the experiment of S. Burger *et al.*, Phys. Rev. Lett. **83**, 5198 (1999), reveal excellent agreement with the observed soliton decay, confirming the crucial role of the thermal cloud in soliton dynamics.

PACS numbers: 03.75.Lm, 05.45.Yv, 67.80.Gb

Bose-Einstein condensates (BECs) in ultracold gases provide an ideal test ground for nonlinear physics. At temperatures close to absolute zero, the condensate can be accurately described by the Gross-Pitaevskii (GP) equation [1], which has the form of a nonlinear Schrödinger equation where the nonlinear term arises from interactions between atoms. A similar equation appears in nonlinear optics, where it is known to support soliton solutions [2]. It is natural, therefore, to expect solitons in BECs.

Both bright and dark solitons have indeed been observed in experiments. Bright solitons can be formed when the atomic interactions are attractive [3, 4, 5], whereas “gap” bright solitons have been created experimentally in repulsive condensates in optical lattices [6]. Repulsive condensates in harmonic traps, however, can only support dark solitons, which correspond to propagating one-dimensional localized minima in the density. Dark solitons have been generated experimentally [7, 8, 9, 10], and their zero temperature properties have been studied theoretically in both three-dimensional geometries, where they exhibit dynamical instabilities [10, 11, 12], as well as in one dimension [13, 14, 15, 16].

Although modelling the condensates at zero temperature provides important insight into dark solitons, in practice experiments are always performed at non-zero temperatures, where the presence of a cloud of non-condensed particles provides a mechanism for the decay of the soliton. Despite the experimental evidence for such dissipative effects, the finite temperature properties of solitons have received relatively little attention. Refs. [17, 18] predicted dissipation at finite temperatures by considering the reflection of excitations from a soliton in a uniform condensate. The role of quantum fluctuations has also been studied [19].

This Letter uses numerical simulations to perform a detailed quantitative study of the dissipative dynamics of dark solitons in elongated harmonic traps at finite temperatures. At zero temperature, a dark soliton is predicted to oscillate in the axial direction [12, 13, 14, 15, 16]. However, the presence of a thermal cloud leads to

damping. As a result, the depth of the propagating soliton decreases in time, leading to an increase in the amplitude of the oscillations, which eventually approaches the half-length of the condensate. This is consistent with a decrease in the soliton energy as a function of time. We perform detailed investigations of this decay for different temperatures and initial soliton depths, and separately assess the role of mean field coupling and binary collisions between the atoms. In particular, we directly simulate the experiment of Burger *et al.* [7], where the evolution of dark solitons, created by phase imprinting, was observed using time-of-flight absorption imaging. Our simulations show that the soliton effectively disappears after only half an oscillation (Fig. 1, bottom images), in good agreement with the experimental findings, thus proving the crucial role of the thermal cloud. This should be contrasted with the undamped dynamics predicted by the GP equation (top images).

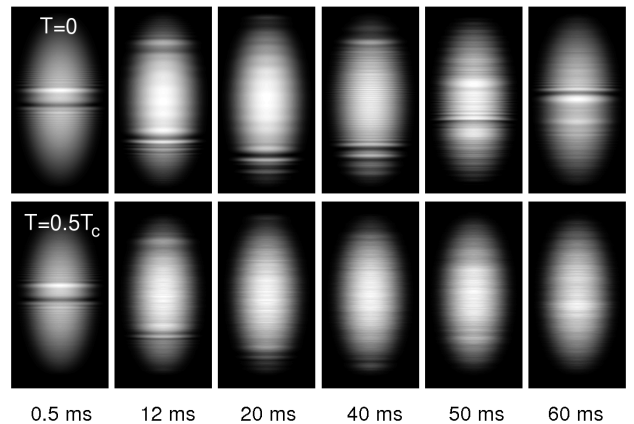


FIG. 1: Evolution of a dark soliton at  $T = 0$  (top) and  $T = 0.5 T_c$  (bottom), corresponding to the experimental parameters of Ref. [7]. In each simulation we initially imprint a phase on the condensate, then allow it to evolve for the time shown before releasing it from the trap. Plotted are condensate column densities after a subsequent expansion of  $t = 4$  ms.

Our simulations are based on the formalism of

Zaremba, Nikuni, and Griffin (ZNG) [20], where the dynamics of the condensate and the thermal cloud are described by the coupled equations:

$$i\hbar \frac{\partial \Psi}{\partial t} = \left( -\frac{\hbar^2 \nabla^2}{2m} + V + gn_c + 2g\tilde{n} - iR \right) \Psi, \quad (1)$$

$$\frac{\partial f}{\partial t} + \frac{\mathbf{p}}{m} \cdot \nabla f - \nabla U \cdot \nabla_p f = C_{12} + C_{22}. \quad (2)$$

Eq. (1) is a generalized GP equation for the condensate wavefunction  $\Psi(\mathbf{r}, t)$ , while Eq. (2) is a Boltzmann equation for the thermal cloud phase space density  $f(\mathbf{p}, \mathbf{r}, t)$  (where  $\mathbf{p}$  is the momentum). The condensate and thermal cloud densities are defined as  $n_c = |\Psi|^2$  and  $\tilde{n} = \int f d^3p/h^3$  respectively, while  $g = 4\pi\hbar^2 a/m$  parameterizes the mean field interactions between atoms of mass  $m$  and scattering length  $a$ . The effective potential is  $U = V + 2g(n_c + \tilde{n})$ , with  $V = m(\omega_\perp^2 r^2 + \omega_z^2 z^2)/2$  representing the harmonic trap. Apart from the mean field coupling between the condensate and non-condensate, Eq. (1) contains a term  $R = (\hbar/2n_c) \int C_{12} d^3p/h^3$  arising from collisional processes,  $C_{12}$ , that add or remove a single particle from the condensate. The  $C_{22}$  term in Eq. (2) denotes binary collisions involving only thermal atoms.

This theory has already been used to model the damping of collective modes, demonstrating good agreement with experiments (see e.g. Ref. [21] and references therein), with the numerical methods used to solve these equations described in Ref. [22]. Here, we also model the dynamics of the thermal cloud using  $N$  body simulations. Eq. (1) is solved in cylindrical coordinates  $(r, z)$  using a Crank-Nicholson scheme, with the singularity in the Laplacian at  $r = 0$  avoided by offsetting the radial grid by half of a grid spacing.

For numerical convenience, our initial analysis is performed for a relatively small sample of  $N = 2 \times 10^4$   $^{87}\text{Rb}$  atoms in a trap with frequencies  $\omega_z = 2\pi \times 10$  Hz and  $\omega_\perp = 2\pi \times 2500$  Hz. The cloud is thus highly elongated along the axial direction, with the tight transverse confinement suppressing “snake-instabilities” which lead to decay of the soliton into vortices [9, 10, 11, 12].

The initial condition for each simulation is established by first self-consistently finding the equilibrium state of the condensate wavefunction and thermal cloud Bose distribution  $f(\mathbf{p}, \mathbf{r}) = \{\exp[(p^2/2m + U - \mu)/k_B T] - 1\}^{-1}$  (where  $\mu$  is the condensate chemical potential) at a given temperature. A soliton is then generated by multiplying the ground state condensate wavefunction  $\Psi(\mathbf{r})$  with  $\Psi_s(z) = \beta \tanh(\beta z/\xi) + i(v/c)$ , where  $\beta = \sqrt{1 - (v/c)^2}$ ,  $\xi = \hbar/\sqrt{mgn_c}$  is the condensate healing length, and  $c = \sqrt{gn_c/(2m)}$  is the speed of sound.

Firstly, we consider only the effect of mean-field coupling  $(n_c, \tilde{n})$  between the condensate and thermal cloud, setting  $R = C_{12} = C_{22} = 0$  in Eq. (2). We perform simulations for a range of initial velocities  $v$ , where smaller

$v$  is associated with deeper solitons (with a completely dark soliton being stationary). To study the soliton decay process in detail, we first consider a rather idealized example of a deep (slow) soliton with  $v = 0.1c$ . The subsequent dynamics is illustrated in Fig. 2, which shows the evolution of the longitudinal density profile for three different temperatures,  $T/T_c$ , where  $T_c$  is the critical temperature for BEC. The density inhomogeneity due to the harmonic trap is evident, with the soliton appearing as a dark line due to its low density.

Fig. 2(a) illustrates the dynamics at  $T = 0$ , where the soliton oscillation has a constant amplitude and a frequency close to  $\omega_z/\sqrt{2}$ , in agreement with the predictions of the GP equation [12, 13, 14]. In this case, the soliton maintains an almost constant depth, and the extrema of the oscillation occur when the density at the soliton minimum reaches zero. Fig. 2(b) shows the result at  $T = 100$  nK ( $0.2T_c$ ), where a small thermal cloud is also present. The steady increase in the oscillation amplitude accompanies a decrease in the soliton depth. At  $T = 200$  nK ( $0.4T_c$ ) [Fig. 2(c)] the rate of increase in amplitude is larger, and the soliton quickly becomes very shallow, making it difficult to visualize in the image.

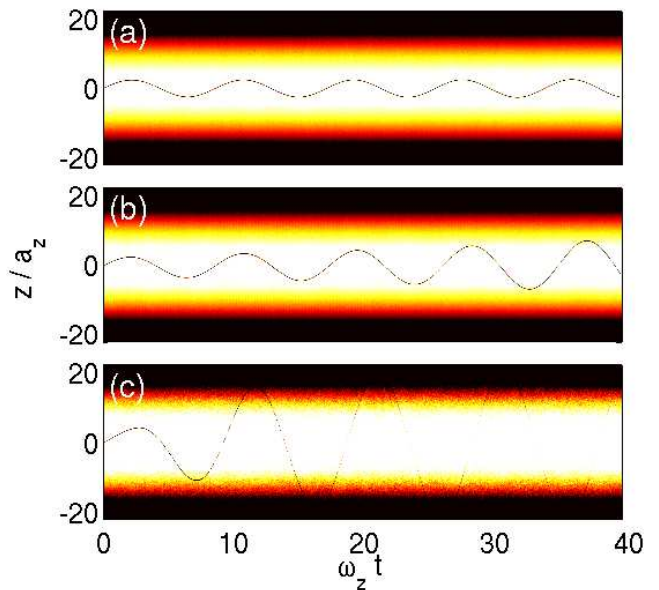


FIG. 2: (Color online) Temporal evolution of the condensate density as a function of  $z$  along a cross-section at  $r = \Delta r/2$ , where  $\Delta r$  is the grid spacing. Light colors represent high densities and dark low densities, with the soliton appearing as a dark line. Both the position and time units are expressed in terms of the axial trap frequency  $\omega_z$ , where  $a_z = [\hbar/(m\omega_z)]^{1/2}$ . The three different plots are for (a)  $T = 0$ , (b)  $T \simeq 0.2T_c$ , and (c)  $T \simeq 0.4T_c$ , where  $T_c \simeq 500$  nK, and the initial velocity is  $v = 0.1c$ .

This increase in oscillation amplitude is a consequence of damping of the soliton due to dissipation. This is most

clearly seen by considering the energy of the soliton

$$E_s(r, t) = \int_{z_s - \delta}^{z_s + \delta} dz \left[ \frac{\hbar^2}{2m} \left| \frac{d\Psi}{dz} \right|^2 + \frac{g}{2} (n_c - n_0)^2 \right], \quad (3)$$

evaluated at  $r = \Delta r/2$ , which is the nearest grid point to the  $z$ -axis. The integral is taken over a small interval  $2\delta$  centered on the soliton position,  $z_s$ , where we choose  $\delta = 5\xi$ . The background density for a condensate without a soliton is represented by  $n_0$ .

In Fig. 3 we plot the soliton energy as a function of time. We see that for  $T = 0$  (dotted black line, top) the energy is constant, apart from an oscillation arising from continuous soliton-sound interactions [15]: an accelerating soliton in a harmonic trap periodically emits sound, leading to an instantaneous loss in energy. However, since the condensate is of finite size, the sound cannot escape from the system and is therefore periodically re-absorbed by the soliton, thus leading to no net decay in energy. In contrast, at finite temperatures there is a gradual loss of energy. While this effect is only marginal at relatively low temperatures ( $T \simeq 0.2T_c$ ) represented by the black solid line, the dissipation is significantly enhanced with increasing temperature, as can be seen from the black dashed line ( $T \simeq 0.4T_c$ ).

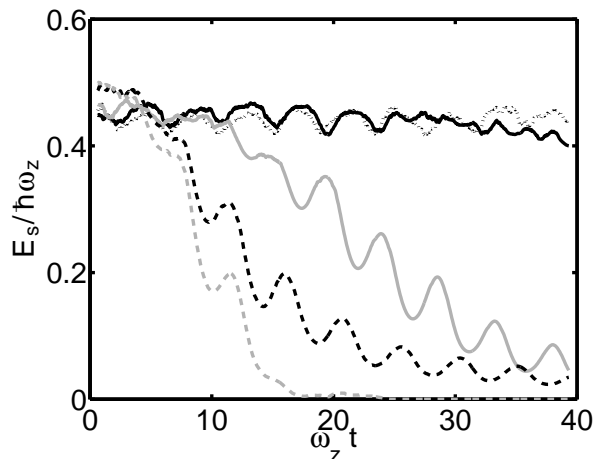


FIG. 3: Soliton energy,  $E_s$ , as a function of time for the parameters of Fig. 2, and temperatures  $T = 0$  (dotted),  $T \simeq 0.2T_c$  (solid) and  $T \simeq 0.4T_c$  (dashed). In the latter two cases, black lines plot the collisionless simulations, while gray lines include collisions.

Although the collisionless regime discussed thus far captures some of the essential physics, experiments with solitons are actually performed in the presence of collisions ( $C_{12} \neq 0$ ,  $C_{22} \neq 0$ ), to which we now turn our attention. The energy decay when collisions are included is represented by the gray lines in Fig. 3. Comparing to the collisionless results, one sees that the decay rate is greatly enhanced, and for  $T \simeq 0.4T_c$  the energy falls to zero already at  $\omega_z t \simeq 20$ .

Simulations for the soliton dynamics have been performed for a range of temperatures, initial velocities, and with and without collisions. In order to quantify the resulting soliton decay, we define a “half-life”,  $\tau_{1/2}$ , which corresponds to the time required for the soliton depth to reach half of its initial value. This quantity is relevant since it is closely related to the contrast of the absorption images obtained experimentally after time-of-flight expansion. The dependence of the half-life on the above parameters is shown in Fig. 4. The procedure for obtaining  $\tau_{1/2}$  is illustrated in the inset, which plots the time-dependence of  $d$ , the depth of the soliton normalized to its initial value. Dashed lines show the point at which  $d = 0.5$  for the first time, while the dotted lines indicate the points at which  $d = 0.45$  and  $d = 0.55$ . These enable us to add error bars to our half-life estimates, in a manner which could account for experimental uncertainties in the contrast of the absorption images. Note that these error bars may be asymmetrical due to the non-monotonic change of the soliton depth arising from soliton-sound interactions.

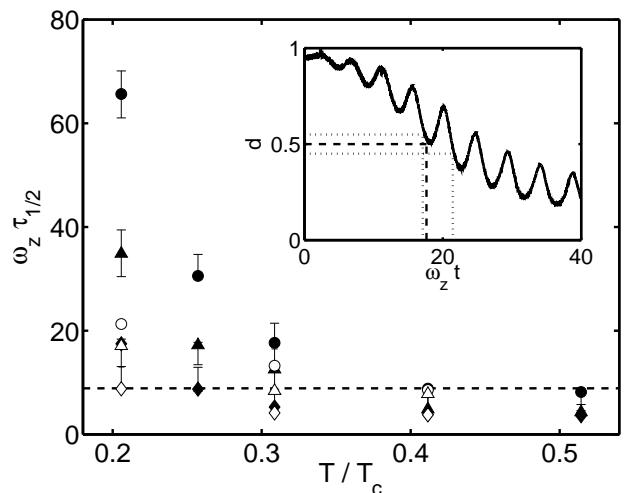


FIG. 4: Time,  $\tau_{1/2}$ , for the soliton depth to decay to half of its initial value as a function of scaled temperature,  $T/T_c$ , for different initial velocities  $v = 0.1c$  (circles),  $v = 0.25c$  (triangles), and  $v = 0.5c$  (diamonds). Solid (open) symbols correspond to collisionless (collisional) simulations. The dashed line marks the period of one soliton oscillation,  $\omega_z t = 2^{3/2}\pi$ . *Inset*: Time-dependence of the soliton depth,  $d$ , scaled to its initial value, for  $T \simeq 0.3T_c$ ,  $v = 0.1c$ , and  $C_{12} = C_{22} = 0$ . This yields  $\tau_{1/2}$  data points for the main graph (dashed lines) and the asymmetrical error bars obtained from  $0.45 < d < 0.55$  (dotted lines).

The main graph in Fig. 4 plots the temperature dependence of the half-lives for different initial soliton speeds. These reveal that the damping time decreases both with increasing temperature, as expected, and increasing initial speed. The half-life is additionally found to decrease when collisions are taken into account, consistent with

the energy decay observed in Fig. 3. The latter change is dramatic for low temperatures and small initial velocities, although the effect of collisions becomes less important at higher temperatures. In particular, at high  $T$  and large initial  $v$ , the half-life is less than the period of the soliton oscillation (marked with a dashed line) even when collisions are absent, indicating that their inclusion will do little to further enhance the decay. Note that the large soliton damping observed here at relatively low temperatures contrasts with the case of collective excitations, where finite  $T$  effects only become important at higher temperatures,  $T > 0.5 T_c$  [21].

This strong damping effect is present even though we have so far considered a rather idealized scenario with a large trap aspect ratio. In experiments the damping may be even more pronounced. To illustrate this, we explicitly consider the parameters of the experiment of Burger *et al.* [7]:  $N = 1.5 \times 10^5$   $^{87}\text{Rb}$  atoms,  $\omega_z = 2\pi \times 14$  Hz,  $\omega_\perp = 2\pi \times 425$  Hz, and  $T \simeq 0.5 T_c$  [18].

Experimentally, a “phase-imprinting” method was used to generate solitons [7], where light was shone on one half of the condensate to create a phase imbalance,  $\Delta\phi$ . To simulate this, we multiply our condensate wavefunction at  $t = 0$  by  $e^{i\phi(z)}$ , where  $\phi(z) = 0$  for  $z < -\ell_e/2$ , and  $\phi(z) = \Delta\phi$  for  $z > \ell_e/2$ . Experimentally, due to diffraction of the light, there is a smooth transition of the phase between the two halves, which takes place over a length of  $\ell_e$ . We represent this transition with a linear ramp,  $\phi = (z/\ell_e + 1/2)\Delta\phi$ , for  $-\ell_e/2 < z < \ell_e/2$ .

A further consideration when simulating the experiment is that the resulting solitons were too small to detect *in situ*, so the condensate was released from the trap and allowed to expand before imaging. We simulate this procedure by allowing the system to evolve in the trap for a variable time after phase imprinting, and subsequently setting the trap potential  $V = 0$ . The column density of the condensate is calculated  $t = 4$  ms later, which simulates a typical absorption image obtained experimentally.

Fig. 1 presents our computed expansion images for  $\ell_e = 1 \mu\text{m}$  and  $\Delta\phi = \pi$ , for the cases of  $T = 0$  (top) and  $T \simeq 0.5 T_c$  (bottom). The corresponding experimental images for the first two columns (i.e. for times  $t \leq 12$  ms) were presented in Ref. [7], where it was argued that the soliton had damped sufficiently to prevent it from being observed at subsequent times. On this timescale, our simulated expansion images at finite  $T$  reveal that the soliton decays to approximately half of its original depth, in agreement with experiment. Moreover, in its subsequent evolution, the soliton spends a large amount of time near the edge of the trap where it is heavily damped. In fact, our finite temperature simulations reveal that the soliton never actually re-emerges from the edge of the trap, in stark contrast to the corresponding prediction of the GP equations (top row of Fig. 1). Given the limited experimental visibility at the edge of the expanded profiles, our findings are thus in good agreement with the experiment

of Ref. [7], as well as with the estimates of Ref. [18].

To conclude, we have studied the dynamics of dark solitons in elongated Bose Einstein condensates using finite temperature simulations. Unlike the undamped soliton oscillations predicted by the Gross-Pitaevskii equation, dissipation arises at finite temperatures, leading to an increase in the oscillation amplitude and a decrease in both the soliton depth and energy. This dissipation increases with temperature and initial velocity, and is in general sensitive to the inclusion of binary collisions between the atoms. Nevertheless, our work indicates that the predicted dark soliton oscillations should be observable in realistic elongated geometries, provided that the temperature is a small fraction of the critical temperature. Direct comparison of our simulations with the experiment of Burger *et al.* [7] shows very good agreement, demonstrating that thermal dissipation fully accounts for the absence of soliton oscillations in this experiment.

This research was supported by EPSRC.

- 
- [1] L. P. Pitaevskii and S. Stringari, *Bose-Einstein Condensation*, Clarendon Press, Oxford (2003).
  - [2] Y. S. Kivshar and B. Luther-Davies, Phys. Rep. **298**, 81 (1998).
  - [3] K. E. Strecker *et al.*, Nature (London) **417**, 150 (2002).
  - [4] L. Khaykovich *et al.*, Science **296**, 1290 (2002).
  - [5] S. L. Cornish, S. T. Thompson, and C. E. Wieman, Phys. Rev. Lett. **96**, 170401 (2006).
  - [6] B. Eiermann *et al.*, Phys. Rev. Lett. **91**, 060402 (2003).
  - [7] S. Burger *et al.*, Phys. Rev. Lett. **83**, 5198 (1999).
  - [8] J. Denschlag *et al.*, Science **287**, 97 (2001).
  - [9] Z. Dutton *et al.*, Science **293**, 663 (2001).
  - [10] B. P. Anderson *et al.*, Phys. Rev. Lett. **86**, 2926 (2001).
  - [11] D. L. Feder *et al.*, Phys. Rev. A **62**, 053606 (2000); J. Brand and W. P. Reinhardt, *ibid.* **65**, 043612 (2002).
  - [12] A. E. Muryshev, H. B. van Linden van den Heuvell, and G. V. Shlyapnikov, Phys. Rev. A **60**, R2665 (1999).
  - [13] Th. Busch and J. R. Anglin, Phys. Rev. Lett. **84**, 2298 (2000).
  - [14] D. J. Frantzeskakis *et al.*, Phys. Rev. A **66**, 053608 (2002); G. Theocharis *et al.*, *ibid.* **72**, 023609 (2005).
  - [15] N. G. Parker *et al.*, Phys. Rev. Lett. **90**, 220401 (2003).
  - [16] V. V. Konotop and L. P. Pitaevskii, Phys. Rev. Lett. **93**, 240403 (2004).
  - [17] P. O. Fedichev, A. E. Muryshev, and G. V. Shlyapnikov, Phys. Rev. A **60**, 3220 (1999).
  - [18] A. E. Muryshev *et al.*, Phys. Rev. Lett. **89**, 110401 (2002).
  - [19] J. Dziarmaga, Z. P. Karkuszewski and K. Sacha, J. Phys. B **36**, 1217 (2003).
  - [20] E. Zaremba, T. Nikuni, and A. Griffin, J. Low. Temp. Phys. **116**, 277 (1999).
  - [21] B. Jackson and E. Zaremba, Phys. Rev. Lett. **88**, 180402 (2002).
  - [22] B. Jackson and E. Zaremba, Phys. Rev. A **66**, 033606 (2002).